High-Resolution Optical Vector Analysis With Enhanced Sensitivity

Ting Qing, Shupeng Li, Yijie Fang, Lihan Wang, Xiaohu Tang, Meihui Cao, Xufeng Chen, Zhaoxin Guo, and Shilong Pan, *Senior Member, IEEE*

***Abstract*— High-resolution and high-sensitivity optical vector analysis (OVA) is highly desired by many applications, such as optical sensors and photonic integrated circuits (PICs). However, it is difficult to achieve high resolution and high sensitivity simultaneously. Here, we propose and experimentally demonstrate a high sensitivity OVA using coherent detection to achieve the complex frequency responses (including magnitude and phase responses) of a device under test (DUT). Carrier phase noise (CPN) cancellation is employed to eliminate the carrier phase fluctuation induced by the coherent detection. In an experiment, the frequency responses of a fiber Bragg grating (FBG) is accurately measured by the proposed method when the probe light is suppressed by ∼18 dB. As a comparison, the method using coherent detection without CPN cancellation can only achieve the magnitude response, and the method using direct detection cannot obtain an effective measurement. The influence of the linewidth and time delay on the measurement is discussed. The proposed OVA provides a stable, high resolution, high sensitivity and low cost approach for characterizing optical devices with arbitrary response, especially for optical devices with large loss or bandpass response.**

***Index Terms*— Frequency response, vector analysis, optical instrument.**

I. Introduction

THE spectral response of an optical component, including magnitude response and phase response, is usually measured by an optical vector analyzer (OVA), which is essential to the development of optical devices and photonic integrated chips (PICs). The early OVA was realized based on the modulation phase-shift method [1] and swept-frequency interferometry [2]. However, both methods rely on a tunable laser source (TLS) for optical frequency scanning, leading to a relatively low resolution (typically 1.6 pm, 200 MHz at 1550 nm). In order to obtain a high-resolution spectral response measurement, OVAs based on multi-frequency modulation [3], [4] or linear-frequency modulation [5] have been proposed. These methods have a typical resolution of 1.6 MHz and can usually perform a measurement in a short time (typically 10 μs), but their dynamic range is relatively low due to the small signal to noise ratio (SNR) of the probe signal. Recently, OVAs based on electro-optic modulation and microwave frequency scanning were proposed to achieve large dynamic range and high resolution at the same time [6]–[20]. Benefitting from the ultrafine frequency scanning of the microwave source, these methods generally have a high resolution (typically 1 MHz). By using an ultra-narrow linewidth laser, we reported an OVA with the highest frequency resolution of 334 Hz [16]. Its dynamic range reached 90 dB. However, due to the employment of direct detection, such high-resolution OVA usually has a low sensitivity. When the probe light is greatly suppressed by the device under test (DUT) with a large loss, such as PICs (typically 20 dB), previous OVAs can hardly measure their responses.

In this paper, we propose a novel OVA with high resolution and high sensitivity based on coherent detection and carrier phase noise cancellation, which employs asymmetric optical double-sideband (ODSB) modulation to improve the measurement bandwidth. Different from previous high-resolution OVAs [9], [16], the proposed method separates the ODSB signal into a local portion and a probe portion. A frequency-shifted carrier is generated after an acousto-optic modulator (AOM). The local portion is directly combined with a part of the frequency-shifted carrier. The probe portion with its magnitude and phase changed by the DUT is combined with the other part of the frequency-shifted carrier. After photodetection, the ratio of the local photocurrent to the probe photocurrent is applied to represent the frequency response of the DUT, which eliminates the carrier phase fluctuation induced by the coherent detection. Here, we name the process carrier phase noise (CPN) cancellation. To demonstrate the feasibility of the proposed OVA, an experiment to characterize the reflection spectrum of a fiber Bragg (FBG) grating is carried out. The return loss of the FBG at the carrier wavelength is about 18 dB. Under such loss, the method using coherent detection without CPN cancellation can only measure the magnitude response, and the method using direct detection obtains an erroneous measurement, while the proposed method can still achieve an accurate measurement with a range of 50 GHz and a frequency setting resolution of 5 MHz. With an enhanced sensitivity, the proposed OVA can measure high-loss optical devices or characterize a bandpass device when the carrier is located at the stop band.

II. Principle

Fig. 1 illustrates the schematic diagram of the OVA based on CPN cancellation. A narrow-linewidth laser source generates

Manuscript received April 9, 2021; accepted April 22, 2021. Date of publication May 5, 2021; date of current version May 11, 2021. This work was supported in part by the National Key R&D Program of China under Grant 2018YFB2201803 and in part by the Postgraduate Research & Practice Innovation Program of Jiangsu Province under Grant KYCX18_0290. *(Corresponding author: Shilong Pan.)*

The authors are with the Key Laboratory of Radar Imaging and Microwave Photonics, Ministry of Education, Nanjing University of Aeronautics and Astronautics, Nanjing 210016, China (e-mail: pans@nuaa.edu.cn).

Color versions of one or more figures in this letter are available at https://doi.org/10.1109/LPT.2021.3075713.

Digital Object Identifier 10.1109/LPT.2021.3075713

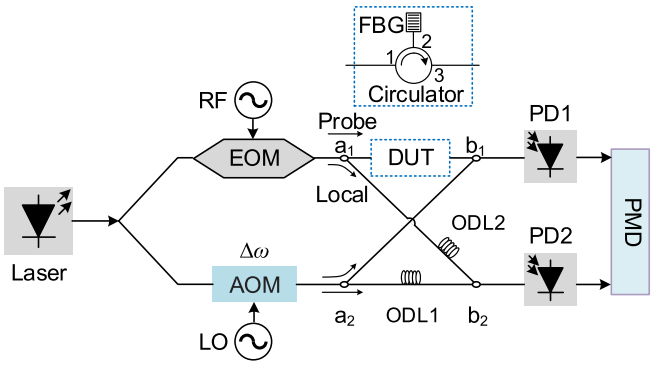

Fig. 1. Schematic diagram of the OVA based on CPN cancellation. EOM, electro-optic modulator; AOM, acousto-optic modulator; DUT, device under test; ODL, optical delay line; PD, photodetector; PMD, phase-magnitude detector; RF, radio frequency; LO, local oscillator.

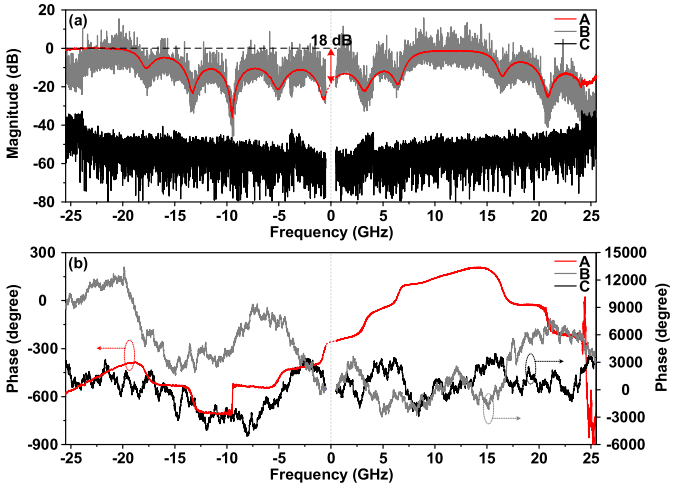

Fig. 2. The measured (a) magnitude and (b) phase responses of the reflection spectrum of an FBG. Trace A, B, and C are measured by the proposed OVA, the ODSB-based OVA using coherent detection without CPN cancellation, and the ODSB-based OVA using direct detection, respectively.

a CW lightwave with a frequency of ω_c. Then, it is split into two portions. One portion is modulated by a sinusoidal signal from an RF source to obtain an ODSB signal. Mathematically, the ODSB signal at point a_1 can be expressed as

$$E_{\mathrm{ODSB}}(t) = \left[A_{-1}e^{-j\omega_m t} + A_0 + A_{+1}e^{j\omega_m t}\right] e^{j[\omega_c t+\phi(t)]}, \quad (1)$$

where ω_m is the frequency of the RF signal, $\phi(t)$ is the phase fluctuation of the optical carrier, $A_{\pm 1}$ and A_0 are the complex amplitudes of the $\pm$1st-order sidebands and the carrier, respectively.

The other portion is frequency shifted at an AOM to achieve an optical reference signal, which can be written as

$$E_R(t) = A_R e^{j[(\omega_c+\Omega)t+\phi(t-\tau_0)]}, \quad (2)$$

where A_R is the complex amplitude, Ω is the frequency shift, τ_0 is the delay difference between point a_1 and point a_2 to the laser source.

The generated ODSB signal and the optical reference signal are divided into two portions, respectively. One portion of the ODSB signal (denoted as the probe signal) is launched into a DUT and combined with a part of the optical reference signal. Thus, the signal at point b_1 can be described as

$$\begin{aligned} E_{b1}(t) = {} & \frac{1}{\sqrt{2}}A_{-1}H(\omega_c-\omega_m)e^{j[(\omega_c-\omega_m)(t-\tau_{a1b1})+\phi(t-\tau_{a1b1})]} \\ & + \frac{1}{\sqrt{2}}A_0 H(\omega_c)e^{j[\omega_c(t-\tau_{a1b1})+\phi(t-\tau_{a1b1})]} \\ & + \frac{1}{\sqrt{2}}A_{+1}H(\omega_c+\omega_m)e^{j[(\omega_c+\omega_m)(t-\tau_{a1b1})+\phi(t-\tau_{a1b1})]} \\ & + \frac{1}{\sqrt{2}}A_R e^{j[(\omega_c+\Omega)(t-\tau_{a2b1})+\phi(t-\tau_0-\tau_{a2b1})]}, \end{aligned} \quad (3)$$

where $H(\omega)$ is the frequency response of the DUT, τ_{ambn} is the time delay from point a_m to point b_n. The other portion of the ODSB signal, after passing through an optical delay line (ODL), is combined with the other part of the optical reference signal. So, the signal at point b_2 is

$$\begin{aligned} E_{b2}(t) = {} & \frac{1}{\sqrt{2}}A_{-1}e^{j[(\omega_c-\omega_m)(t-\tau_{a1b2})+\phi(t-\tau_{a1b2})]} \\ & + \frac{1}{\sqrt{2}}A_0 e^{j[\omega_c(t-\tau_{a1b2})+\phi(t-\tau_{a1b2})]} \\ & + \frac{1}{\sqrt{2}}A_{+1}e^{j[(\omega_c+\omega_m)(t-\tau_{a1b2})+\phi(t-\tau_{a1b2})]} \\ & + \frac{1}{\sqrt{2}}A_R e^{j[(\omega_c+\Omega)(t-\tau_{a2b2})+\phi(t-\tau_0-\tau_{a2b2})]}. \end{aligned} \quad (4)$$

After photodetection, two photocurrents are generated and received by a multi-channel phase-magnitude detector (PMD), simultaneously. Since the PMD is set to receive signals with frequencies of $\omega_m \pm \Omega$, the relevant components of the photocurrents are (5), as shown at the bottom of the next page, where η_1 and η_2 are the responsitivity of the PD1 and the PD2, respectively.

To eliminate the influence of the phase fluctuation $\phi(t)$, we employ two ODLs to make $\tau_{a1b1} \approx \tau_{a1b2}$, and $\tau_{a2b1} = \tau_{a2b2}$. Considering that the phase fluctuation $\phi(t)$ is relatively slow duo to the narrow linewidth of the laser source, $\phi(t-\tau_{a1b1}) \approx \phi(t-\tau_{a1b2})$, and $\phi(t-\tau_0-\tau_{a2b1}) = \phi(t-\tau_0-\tau_{a2b2})$ can be obtained. Then, the DUT response can be achieved by Fourier transform of the photocurrents from PD1 and PD2:

$$\begin{aligned} H(\omega_c-\omega_m) &= \left(\frac{\eta_2 i_{PD1}(\omega_m+\Omega)}{\eta_1 i_{PD2}(\omega_m+\Omega)}\right)^* \cdot \exp(j\Delta\varphi) \\ H(\omega_c+\omega_m) &= \frac{\eta_2 i_{PD1}(\omega_m-\Omega)}{\eta_1 i_{PD2}(\omega_m-\Omega)} \cdot \exp(-j\Delta\varphi), \end{aligned} \quad (6)$$

where $\Delta\varphi$ is the residual phase fluctuation induced by the mismatch between τ_{a1b1} and τ_{a1b2}. It should be noted that τ_{a1b1} includes the frequency dependence of the DUT, which cannot be set arbitrarily equal to τ_{a1b2}. However, considering that the DUT delay variation is difficult to exceed ns lever, the residual phase fluctuation $\Delta\varphi$ can be ignored when a narrow-linewidth laser source is employed.

It should be noted that, before measuring a DUT, a normalization calibration must be performed to remove the system response [16].

III. Experimental Results And Discussions

An experiment is performed according to the setup illustrated in Fig. 1. A tunable narrow-linewidth laser source

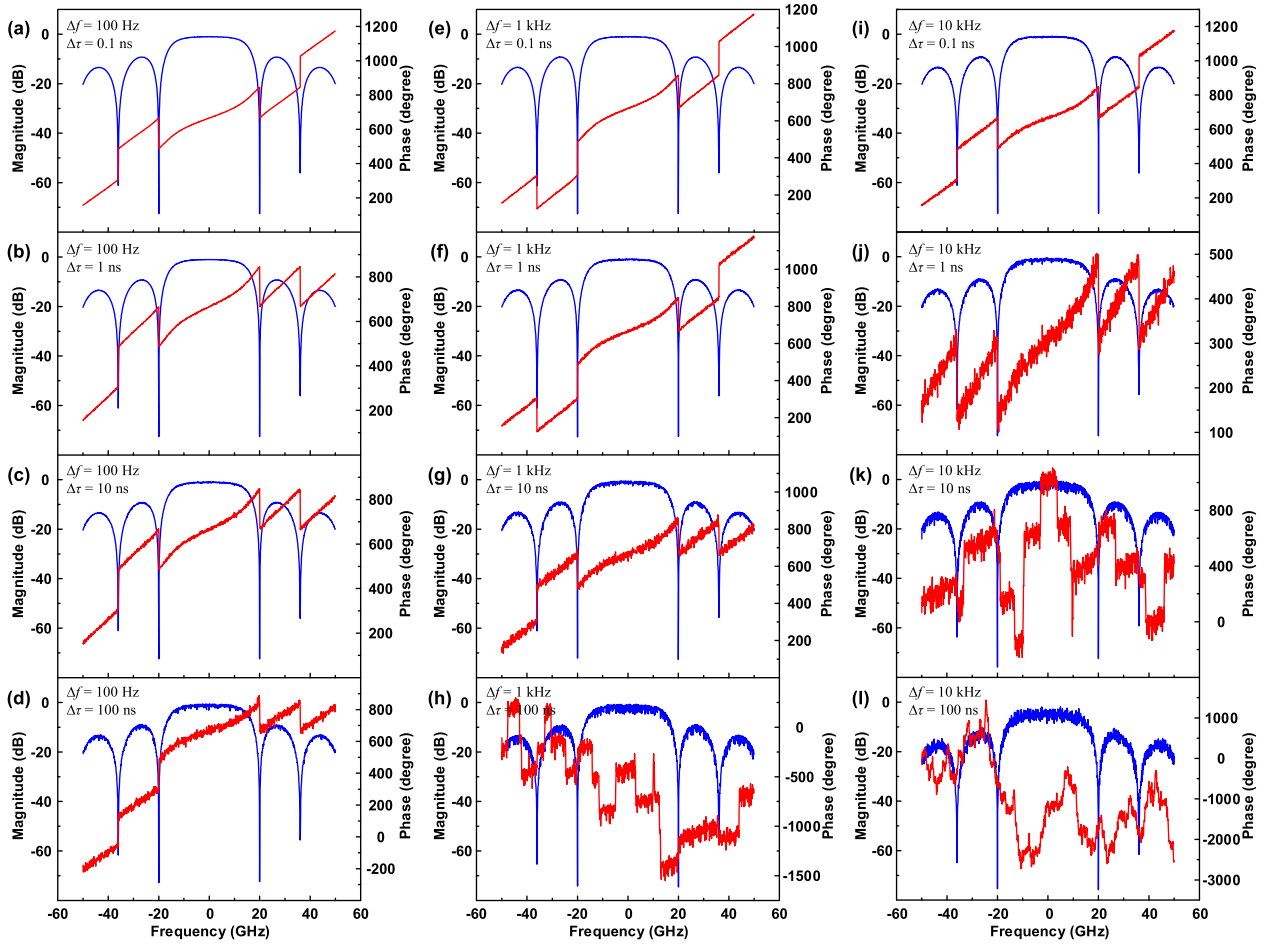

Fig. 3. Simulated measurement of a uniform FBG. (a-l) The linewidth is 100 Hz, 1 kHz, and 10 kHz, respectively. The residual delay is 0.1 ns, 1ns, 10ns, and 100 ns, respectively. The blue traces represent magnitude responses. The red traces are phase responses.

module (TeraXion PS-TNL, the linewidth is ∼1 kHz) is employed to produce an optical carrier with low phase noise. Then, the carrier is split into two parts. One part is modulated at a Mach-Zehnder modulator (Fujitsu FTM7938EZ) to obtain an ODSB signal. The other portion is frequency shifted at an AOM (Gooch&Housego Inc.), driven by an RF signal with a frequency of 80 MHz. The respective optical path differences of the two MZ interferometers are adjusted to the same by two manual variable ODLs (General Photonics VDL-001). An FBG is used as the DUT. Two photodetectors (Finisar XPDV2120RA) are exploited to convert the optical signal into a photocurrent. A 4-port electrical vector network analyzer (EVNA, R&S ZVA67) is used as the microwave source and the phase-magnitude detector.

The reflection spectrum of the FBG is measured by three kinds of OVAs, including the proposed OVA, the ODSB-based OVA using coherent detection without CPN cancellation [9], and the ODSB-based OVA using direct detection [16]. Fig. 2 shows the measured frequency responses. The microwave source is set to sweep from 0.5 to 25.5 GHz, and the number of the frequency points is 5001. Thus, 50-GHz measurement bandwidth and 5-MHz frequency setting resolution are achieved. The residual delay between τ_{a1b1} and τ_{a1b2} is ∼1.3 ns, induced by the FBG. It can be seen that the measurement uncertainty of the proposed OVA is very small, and the measured results (i.e., trace A) can well characterize the FBG reflection spectrum. If using coherent detection but without CPN cancellation, the ODSB-based

$$
\begin{aligned}
i_{\mathrm{PD1}}(\omega_{\mathrm{m}}+\Omega,t) &= \frac{1}{2}\eta_1 A_{-1}^{*} A_R H^{*}(\omega_{\mathrm{c}}-\omega_{\mathrm{m}})\cdot e^{j[(\omega_{\mathrm{m}}+\Omega)t+\omega_{\mathrm{c}}(\tau_{\mathrm{a1b1}}-\tau_{\mathrm{a2b1}})-\omega_{\mathrm{m}}\tau_{\mathrm{a1b1}}-\Omega\tau_{\mathrm{a2b1}}+\phi(t-\tau_0-\tau_{\mathrm{a2b1}})-\phi(t-\tau_{\mathrm{a1b1}})]} \\
i_{\mathrm{PD1}}(\omega_{\mathrm{m}}-\Omega,t) &= \frac{1}{2}\eta_1 A_{+1} A_R^{*} H(\omega_{\mathrm{c}}+\omega_{\mathrm{m}})\cdot e^{j[(\omega_{\mathrm{m}}-\Omega)t-\omega_{\mathrm{c}}(\tau_{\mathrm{a1b1}}-\tau_{\mathrm{a2b1}})-\omega_{\mathrm{m}}\tau_{\mathrm{a1b1}}+\Omega\tau_{\mathrm{a2b1}}-\phi(t-\tau_0-\tau_{\mathrm{a2b1}})+\phi(t-\tau_{\mathrm{a1b1}})]} \\
i_{\mathrm{PD2}}(\omega_{\mathrm{m}}+\Omega,t) &= \frac{1}{2}\eta_2 A_{-1}^{*} A_R\cdot e^{j[(\omega_{\mathrm{m}}+\Omega)t+\omega_{\mathrm{c}}(\tau_{\mathrm{a1b2}}-\tau_{\mathrm{a2b2}})-\omega_{\mathrm{m}}\tau_{\mathrm{a1b2}}-\Omega\tau_{\mathrm{a2b2}}+\phi(t-\tau_0-\tau_{\mathrm{a2b2}})-\phi(t-\tau_{\mathrm{a1b2}})]} \\
i_{\mathrm{PD2}}(\omega_{\mathrm{m}}-\Omega,t) &= \frac{1}{2}\eta_2 A_{+1} A_R^{*}\cdot e^{j[(\omega_{\mathrm{m}}-\Omega)t-\omega_{\mathrm{c}}(\tau_{\mathrm{a1b2}}-\tau_{\mathrm{a2b2}})-\omega_{\mathrm{m}}\tau_{\mathrm{a1b2}}+\Omega\tau_{\mathrm{a2b2}}-\phi(t-\tau_0-\tau_{\mathrm{a2b2}})+\phi(t-\tau_{\mathrm{a1b2}})]}
\end{aligned}
\tag{5}
$$

OVA [9] can only achieve an effective magnitude response (i.e., trace B in Fig. 2(a)). It is because that the carrier phase noise is transferred to the photocurrent after coherent detection, which makes the EVNA unable to extract a stable phase response. Due to the CPN induced by the carrier phase noise, the spectrum width of the photocurrent is broadened to be wider than the employed IF bandwidth, leading to a huge magnitude uncertainty (∼20 dB). Thus, trace B cannot show any detailed information, although it has almost the same ups and downs as trace A. If using a wide IF bandwidth, the magnitude uncertainty can be reduced, but the frequency resolution will be limited. In addition, Fig. 2(a) shows two passbands and some sidelobes beside the passband. Since the carrier is not at the passband of the FBG and is suppressed by a sidelobe, the FBG return loss at the carrier frequency reaches ∼18 dB. The optical power of the returned probe signal is only about -20 dBm. If using direct detection, the generated photocurrent will be lower than the noise floor of the PMD. Thus, the ODSB-based OVA using direct detection [16] cannot perform an effective measurement in this case. Trace C in Fig. 2(a) measured by this OVA only represents the noise floor, providing no useful information. Thus, the proposed OVA can detect weak signal and has a high sensitivity.

As can be seen from the experimental results, the CPN cancellation is indispensable for OVAs using coherent detection. To evaluate the influence of CPN cancellation on the phase response measurement, a simulation is performed. The carrier phase noise is modeled using the probability density function:

$$f(\Delta\phi) = \frac{1}{2\pi\sqrt{\Delta f\,\Delta\tau}} \exp\left(-\frac{\Delta\phi^2}{4\pi\,\Delta f\,\Delta\tau}\right), \tag{7}$$

where $\Delta\phi$ is the phase difference between two successive time instants, $\Delta\tau$ is the residual delay, Δf is the TLS linewidth. Fig. 3 shows the simulated results. The IF bandwidth is 100 kHz, Δf is 100 Hz, 1 kHz, and 10 kHz, respectively, and $\Delta\tau$ is 0.1 ns, 1ns, 10ns, and 100 ns, respectively. As can be seen, the measurement uncertainty in the magnitude and phase responses becomes significant as the linewidth and residual delay increase. In severe cases, we cannot achieve an effective phase response, which indicates that the CPN cancellation is ineffective. To reduce the measurement uncertainty, an ultra-narrow linewidth laser should be employed and accurate time delay matching should be performed.

IV. Conclusion

A novel OVA based on CPN cancellation is proposed to achieve high-resolution and high sensitivity simultaneously. The reflection spectrum of an FBG, including the magnitude and phase responses, is obtained when the probe light is suppressed by ∼18 dB, which shows that the proposed OVA has a high sensitivity. The measurement bandwidth is 50 GHz, and the frequency resolution is 5 MHz. The influence of the carrier phase fluctuation and the residual delay on the measurement uncertainty is investigated through simulation, indicating that the delay of the measurement path and the reference path should be well matched to achieve high precision. If using an ultra-narrow linewidth laser, the measurement uncertainty can be further reduced. With a high sensitivity, optical devices with large loss or bandpass response can be accurately measured by the proposed OVA.

References

[1] T. Niemi, M. Uusimaa, and H. Ludvigsen, "Limitations of phase-shift method in measuring dense group delay ripple of fiber Bragg gratings," *IEEE Photon. Technol. Lett.*, vol. 13, no. 12, pp. 1334–1336, Dec. 2001.

[2] D. K. Gifford, B. J. Soller, M. S. Wolfe, and M. E. Froggatt, "Optical vector network analyzer for single-scan measurements of loss, group delay, and polarization mode dispersion," *Appl. Opt.*, vol. 44, no. 34, pp. 7282–7286, 2005.

[3] B. Guo *et al.*, "Characterization of passive optical components with ultra-fast speed and high-resolution based on DD-OFDM," *Opt. Exp.*, vol. 20, no. 20, pp. 22079–22086, 2012.

[4] C. Jin *et al.*, "High-resolution optical spectrum characterization using optical channel estimation and spectrum stitching technique," *Opt. Lett.*, vol. 38, no. 13, pp. 2314–2316, 2013.

[5] S. P. Li, M. Xue, T. Qing, C. Y. Yu, L. G. Wu, and S. L. Pan, "Ultrafast and ultrahigh-resolution optical vector analysis using linearly frequency-modulated waveform and dechirp processing," *Opt. Lett.*, vol. 44, no. 13, pp. 3322–3325, 2019.

[6] Z. Tang, S. Pan, and J. Yao, "A high resolution optical vector network analyzer based on a wideband and wavelength-tunable optical single-sideband modulator," *Opt. Exp.*, vol. 20, no. 6, pp. 6555–6560, 2012.

[7] W. Li, W. T. Wang, L. X. Wang, and N. Zhu, "Optical vector network analyzer based on single-sideband modulation and segmental measurement," *IEEE Photon. J.*, vol. 6, no. 2, Apr. 2014, Art. no. 7901108.

[8] S. Pan and M. Xue, "Ultrahigh-resolution optical vector analysis based on optical single-sideband modulation," *J. Lightw. Technol.*, vol. 35, no. 4, pp. 836–845, Feb. 15, 2017.

[9] T. Qing, M. Xue, M. H. Huang, and S. L. Pan, "Measurement of optical magnitude response based on double-sideband modulation," *Opt. Lett.*, vol. 39, no. 21, pp. 6174–6176, 2014.

[10] W. Jun *et al.*, "Optical vector network analyzer based on double-sideband modulation," *Opt. Lett.*, vol. 42, no. 21, pp. 4426–4429, 2017.

[11] Q. Wang, W.-T. Wang, W. Chen, J.-G. Liu, and N.-H. Zhu, "Optical vector network analyzer with an improved dynamic range based on a polarization multiplexing electro-optic modulator," *Chin. Phys. Lett.*, vol. 34, no. 5, May 2017, Art. no. 054205.

[12] S. Liu, M. Xue, J. Fu, L. Wu, and S. Pan, "Ultrahigh-resolution and wideband optical vector analysis for arbitrary responses," *Opt. Lett.*, vol. 43, no. 4, pp. 727–730, 2018.

[13] M. Xue, S. Liu, and S. Pan, "High-resolution optical vector analysis based on symmetric double-sideband modulation," *IEEE Photon. Technol. Lett.*, vol. 30, no. 5, pp. 491–494, Mar. 1, 2018.

[14] N. Kukharchyk *et al.*, "Optical vector network analysis of ultranarrow transitions in $^{166}Er^{3+}$:$^{7}LiYF_4$ crystal," *Opt. Lett.*, vol. 43, no. 4, pp. 935–938, 2018.

[15] Z. Chen *et al.*, "Long-term measurement of high Q optical resonators based on optical vector network analysis with Pound Drever Hall technique," *Opt. Exp.*, vol. 26, no. 21, pp. 26888–26895, 2018.

[16] T. Qing, S. Li, Z. Tang, B. Gao, and S. Pan, "Optical vector analysis with attometer resolution, 90-dB dynamic range and THz bandwidth," *Nature Commun.*, vol. 10, no. 1, p. 5135, Dec. 2019.

[17] J. Wen *et al.*, "Accuracy-enhanced wideband optical vector network analyzer based on double-sideband modulation," *J. Lightw. Technol.*, vol. 37, no. 13, pp. 2920–2926, Jul. 1, 2019.

[18] J. Dai, Z. Chen, X. Wang, L. Ye, T. Zhang, and K. Xu, "Accurate optical vector network analyzer based on optical double-sideband suppressed carrier modulation," *Opt. Commun.*, vol. 447, pp. 61–66, Sep. 2019.

[19] O. Morozov *et al.*, "Ultrahigh-resolution optical vector analyzers," *Photonics*, vol. 7, no. 1, p. 14, Jan. 2020.

[20] B. Wang, W. Zhang, and X. Fan, "Self-calibrated optical vector analyzer with a largely extended measurement range based on linearly frequency-modulated waveform and recirculating frequency shifter," *Opt. Exp.*, vol. 28, no. 19, pp. 28536–28547, 2020.